Доклади на Българската академия на науките
Comptes rendus de l'Académie bulgare des Sciences
Tome 66, No 1, 2013

SCIENCES ET INGENIERIE
Mécanique

SHOCK-WAVE PROCESSES MODELLING ON RAILWAY VEHICLES USING A SCALED MODEL UTILIZING VISCOELASTIC PROPERTIES

Alexander Kazakoff, Boycho Marinov

(*Submitted by Academician Ya. Ivanov on June 25, 2012*)

Abstract

The shock impacts on the railway vehicles with two-stage spring suspension excite in working mode. These impacts change the kinematics components of the movement, i.e. linear and angular speeds at the end of the shock process and free damped vibrations of the mechanical system arise. In this paper, our aim is to perform a dynamic scaling of the original model in order to build up a new double mass model utilizing viscoelastic properties which is smaller with small masses and is easier to work even possible in laboratory conditions. The new dynamically scaled model is supposed to perform the same behaviour as the original one if its natural frequencies are the same with the original model. The two masses M_1 and M_2 of the new double mass scaled utilizing viscoelastic properties model are calculated after optimization performed with numerical calculations of the characteristic polynomial varying with masses in order to fit the same natural frequencies. The objective of the work presented in this paper is to model the shock-vibrations response of the railway vehicle using a scaled model utilizing viscoelastic properties and to compare the results derived here with the results obtained using the original model.

Key words: shock-vibrations response, shock impacts, carriage, bogie, railway vehicles, dynamic scaling, viscozoelastic properties, frequency analysis, mode shapes, finite element method, numerical analysis

1. Introduction. In this paper the influence of the shock impacts on the railway vehicles with two-stage spring suspension is analyzed. These impacts are excited in working mode when the transport vehicle passes through the splice of the rails. Shock loads arise as a result of this process. They load up the railway

vehicles and change the kinematics components of the movement – linear and angular speeds.

Originally, three technical studies [14–16] were used as a scientific background for the up to date investigation. The original analytical models were derived in [15, 16] and the whole analytical study was summarized in [17]. The 3D finite element method "benchmark" model was analyzed and reported before [14]. The "benchmark" model which is used as a basic cell for the building up of the scaled model was investigated and reported before [14]. The "benchmark" model utilizes viscoelastic properties of rubber is shown in [14]. The free damped vibrations are investigated and reported before [15–17]. These vibrations arise in consequence of the shock impacts [17].

The mechanical system has final number degrees of freedom. The movement of the system is described with the same number generalized co-ordinates. The integration constants are determined by the initial conditions, i.e. from the state of the system at the end of the shock impact [15, 16]. The analysis of the received decision allows determining the action of the impulses on the basic elements of the railway vehicles. It is investigated in what way these basic elements, like springs and dampers, react to the shock-wave processes so that the normal work of transport vehicle in working mode to be guaranteed.

In the present paper, our aim is to perform a dynamic scaling of the original model in order to build up a new double mass model utilizing viscoelastic properties which is smaller with small masses and is easier to work with even in laboratory conditions. The new dynamically scaled model is supposed to perform the same behaviour as the original one, if its natural frequencies are the same with the original model. The two masses M_1 and M_2 of the new model, the adduced masses of the bogie and the carriage, respectively are calculated after optimization performed with calculations of the system characteristic polynomial varying with masses in order to fit the same natural frequencies. In this way, the dynamically scaled model is built up out of the so called "benchmark" model, reported before [14]. The natural frequencies of the scaled model after performing a modal analysis are presented on Table 1.

The objective of the work, presented in this paper is to model the shock-vibrations response of the railway carriage using a scaled double mass dynamic model utilizing viscoelastic properties and to compare the results derived here with the results obtained previously using the original model.

2. The shock-vibrations response. The railway vehicle performs free damped vibrations, analyzed in [15, 16] as a result of the shock impacts. These vibrations are investigated through the dynamic model shown in Fig. 1 [15–17]. We define the following symbols: m_a, J_{ay}, m_b, J_{by}, m_w, J_{wy} are the masses and the mass inertia moments of the axle shaft, the frame of the bogie and the crate of the carriage, respectively, $2l_b$ and $2l_w$ are the bases of the bogie and the crate of the carriage, respectively, $2L_w$ and $2H_w$ are the length and the height of the

Table 1

List of resonant frequencies

Mode No	Frequency [s^{-1}]	Frequency [Hz]	Period [s]
1	1.2501	0.19895	5.0263
2	1.8693	0.29752	3.3612
3	2.4408	0.38846	2.5743
4	6.6263	1.0546	0.94821
5	7.1558	1.1389	0.87806
11	40.284	6.4113	0.15597

crate. The elastic constants of the spring suspension and the damping coefficients are marked with c_b, c_w, β_b, β_w. The vertical displacement of the mass centres of the bogies and the crate of the carriage are marked with z_{bj} $(j = 1, 2)$ and z_w. The angular rotations of the bogies and the crate are marked with φ_{bj} $(j = 1, 2)$ and φ_w.

A current position of the mechanical system is presented for this investigation. The dynamic deflections of the springs in the central part z_j $(j = 1, 2)$ and the axle-box part z_{ij} $(i = 1, 2\ j = 1, 2)$ are determined by the following dependences [1]:

$$
\begin{aligned}
&z_1 = z_w + l_w\varphi_w - z_{b1}, \quad && z_2 = z_w - l_w\varphi_w - z_{b2},\\
&z_{11} = z_{b1} + l_b\varphi_{b1}, && z_{12} = z_{b1} - l_b\varphi_{b1},\\
&z_{21} = z_{b2} + l_b\varphi_{b2}, && z_{22} = z_{b2} - l_b\varphi_{b2},
\end{aligned}
\tag{1}
$$

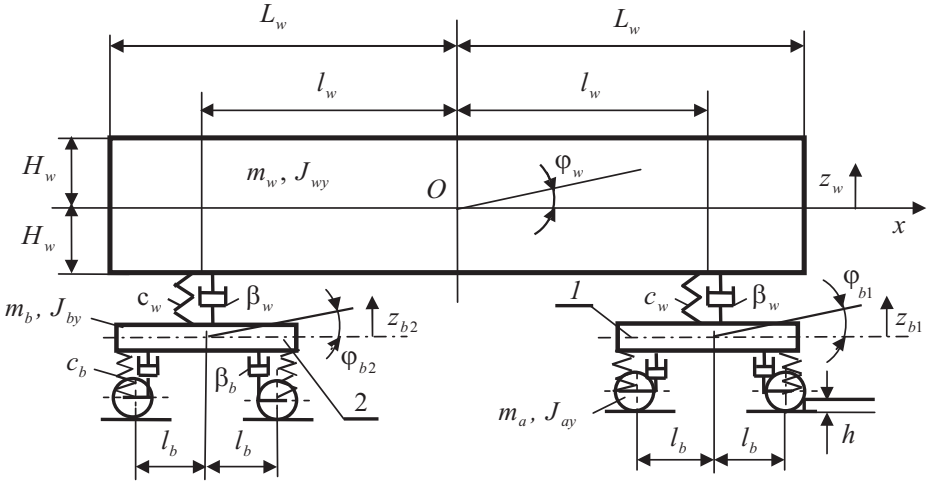

Fig. 1. Dynamic model – the originally defined one

3. Numerical solution. The results of the shock-vibration process are shown below [15–17], in expressions (2)

$$
\begin{array}{lll}
\dot{z}_{b1(0)} = 0.136 \text{ [m/s]}, & \dot{z}_{w(0)} = 0.04 \text{ [m/s]}, & \dot{z}_{b2(0)} = 0.086 \text{ [m/s]}, \\
\dot{\varphi}_{b1(0)} = 0.11 \text{ [s}^{-1}\text{]}, & \dot{\varphi}_{w(0)} = 0.006 \text{ [s}^{-1}\text{]}, & \dot{\varphi}_{b2(0)} = 0, \\
z_{b1(0)} = 0.0027 \text{ [m]}, & z_{w(0)} = 0, & z_{b2(0)} = 0, \\
\varphi_{b1(0)} = 0.0026 \text{ [rad]}, & \varphi_{w(0)} = 0, & \varphi_{b2(0)} = 0.
\end{array} \tag{2}
$$

In this case the following input data are used [1, 2, 6]:

$$
\begin{array}{ll}
c_w = 0.86 \times 10^6 \text{ [N/m]}, & c_b = 1.7 \times 10^6 \text{ [N/m]}, \\
\beta_w = 75 \times 10^3 \text{ [Ns/m]}, & \beta_b = 50 \times 10^3 \text{ [Ns/m]}, \\
l_w = 8.6 \text{ [m]}, & l_b = 1.25 \text{ [m]}, \\
m_w = 28000 \text{ [kg]}, & m_b = 2600 \text{ [kg]}, \\
J_{wy} = 15.4 \times 10^5 \text{ [kg m}^2\text{]}, & J_{by} = 4000 \text{ [kg m}^2\text{]}.
\end{array} \tag{3}
$$

3.1. Stiffness determination of the "benchmark" model. The stiffness determination of the cylindrical body manufactured of rubber [14] is defined by the formula

$$K = E\frac{A}{L}, \tag{4}$$

where E is the Young's modulus, A is the cross sectional area, L is the height of the rubber cylinder. Formula (4) considering the shape of the rubber body can be rewritten in the following way:

$$K^* = K(1 + \beta s^2) = E\frac{A}{L}(1 + \beta s^2), \tag{5}$$

where $\beta = 2$ is a numerical constant, s is the shape factor.

In this equation, the so-called shape factor s is equal to the ratio of the area of one loaded surface to the total force-free area. The shape factor of a rubber cylinder of diameter D and height L, for example, is equal to $\dfrac{D}{4L}$. We can perform the following calculations:

$$A = \pi\frac{D^2}{4} = \pi\frac{0.065^2}{4} = 0.0033 \text{ [m}^2\text{]}, \quad s = \frac{D}{4L} = \frac{1}{4} = 0.25, \tag{6}$$

where $L = 0.065$ [m], $D = 0.065$ [m].

$$K^* = E\frac{A}{L}(1 + \beta s^2) = 3.1 \times 10^5(1 + 2 \times 0.25^2) = 3.4875 \times 10^5 \text{ [N/m]}. \tag{7}$$

The model, presented in Fig. 1, can be equivalent to a double mass dynamic model with first mass $m_1 = 2m_b = 5200$ [kg] and second mass $m_2 = m_w = 28\,000$ [kg]. The two stiffnesses of the suspension shown in Fig. 1 are:

$$
\begin{array}{l}
c_1 = 4c_b = 4 \times 1.7 \times 10^6 = 68 \times 10^5 \text{ [N/m]}, \\
c_2 = 2c_w = 2 \times 0.86 \times 10^6 = 17.2 \times 10^5 \text{ [N/m]}.
\end{array} \tag{8}
$$

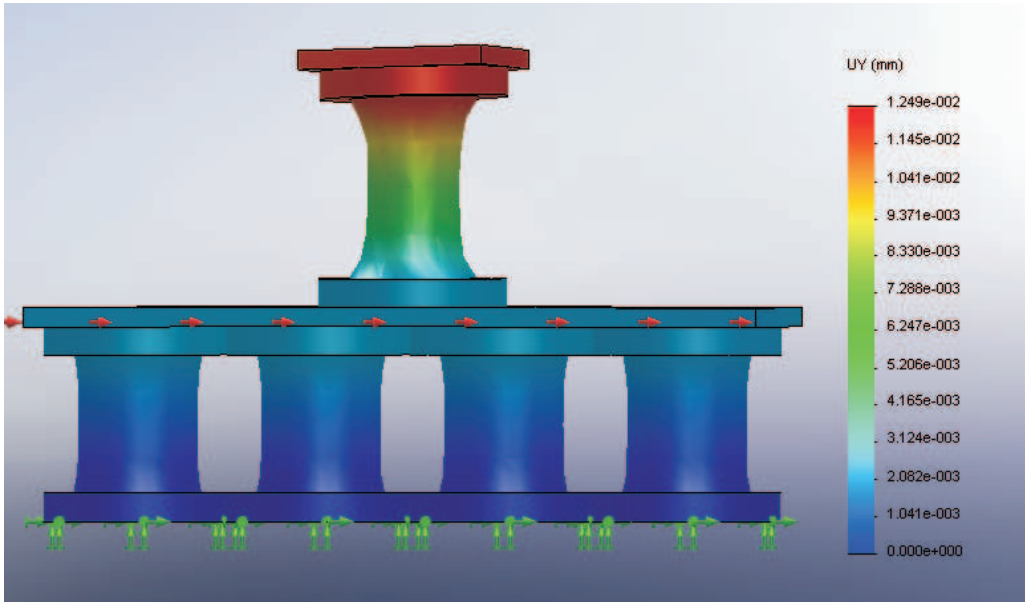

Fig. 2. Displacement plot of the dynamically scaled model

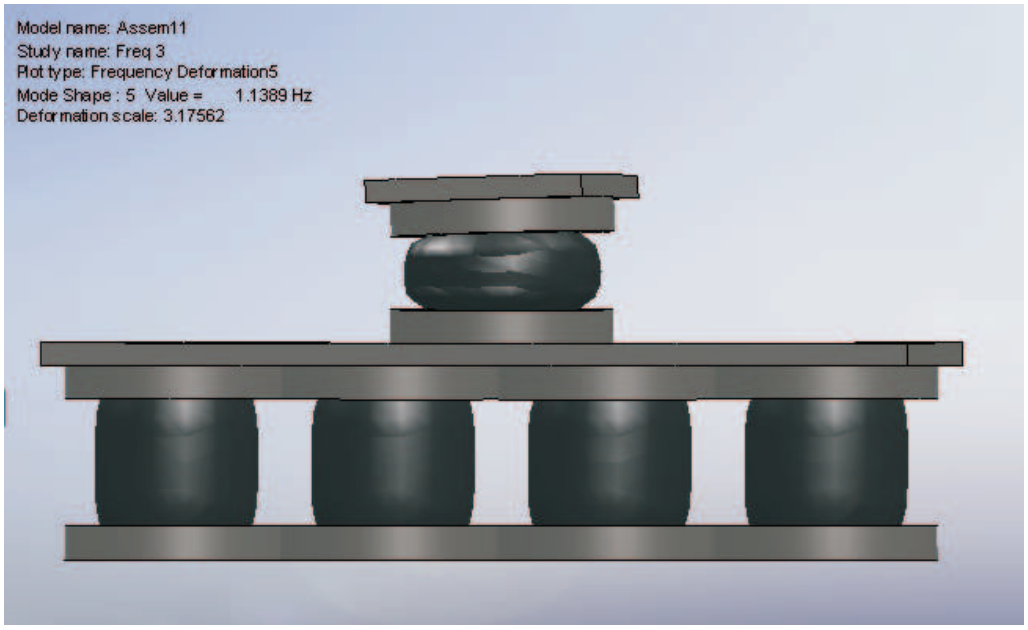

Fig. 3. Deformation plot – mode shape 5 of the dynamically scaled model

3.2. Natural frequencies determination of the "benchmark" model. The two mutually related natural frequencies can be calculated using the characteristic polynomial of the system differential equations, shown below [3–5]

$$\Delta = (c_1 + c_2 - m_1\omega^2)(c_2 - m_2\omega^2) - c_2^2. \tag{9}$$

The two natural frequencies after calculation are derived below [7, 8, 15]

$$\omega_1 = 6.9748 \ [\mathrm{s}^{-1}], \quad \omega_2 = 40.6355 \ [\mathrm{s}^{-1}]. \tag{10}$$

Now, our aim is to perform a dynamic scaling of the model, shown in Fig. 1, in order to build up a new double mass model which is smaller with small masses and is easier to work with even in laboratory conditions. The new dynamically scaled model is supposed to perform the same behaviour as the original if its natural frequencies are the same with the model shown in Fig. 1. The two masses M_1 and M_2 of the new model are calculated after optimization performed with calculations of the characteristic polynomial (9) varying with two masses in order to fit the same natural frequencies and being equal to:

$$M_1 = 1300 \ [\mathrm{kg}], \quad M_2 = 6500 \ [\mathrm{kg}]. \tag{11}$$

In this way, the dynamically scaled model is build up out of the so-called "benchmark" model and presented in Figs 2 and 3. The natural frequencies of the scaled model after performing a modal analysis are presented in Table 1, listed below. The two mode shapes 5 and 11 correspond to the main resonant bouncing frequencies and the mode shape of frequency mode No 5 is presented in Fig. 3.

Dynamic analysis is performed using the scaled model presented in Fig. 2 and the amplitudes of displacements and velocities of the two masses M_1 and M_2 are calculated and shown in Fig. 4.

The scaled model is build up of a construction which is a combination of four "benchmark" models at the basis and one on the top in order to fit the desired natural frequencies. The plate between the two levels is the mass (scaled) of the bogie, which is adjusted by means of the proper density with the mass M_1 and the volume of the intermediate plate. In the same way, the mass of the carriage crate M_2 is presented as the mass (scaled) of the plate on the top. This mass is adjusted by means of the definition of the proper density defined by the mass over the volume of the plate. As it is mentioned above, the two main frequencies and the corresponding bouncing shapes are No 5 and 11 on Table 1 and we should expect the two bodies' motion to be in the same quality, as it is shown in Fig. 3. That is why the displacement plots shown in Fig. 2, we can consider as correct, corresponding to the bouncing motion of the model (see Fig. 3). Here, we must clearly point out that in this study we investigate only the shock impact, not the motion as a whole. The displacement plot – amplitude of displacement is shown

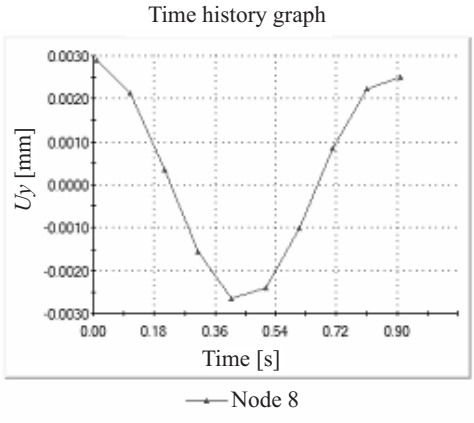

a) Response graph of the displacement of the bogie at node 8 in the middle of mass M_1

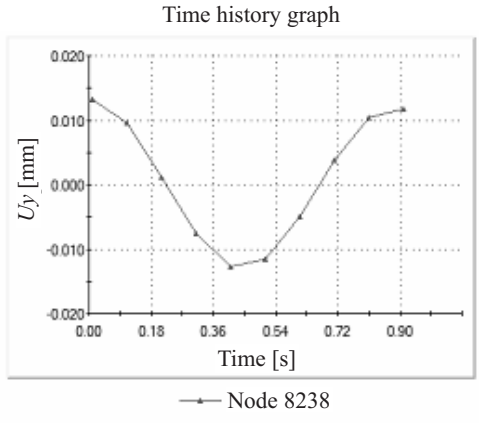

b) Response graph of the displacement of the carriage at node 8238 in the middle of mass M_2

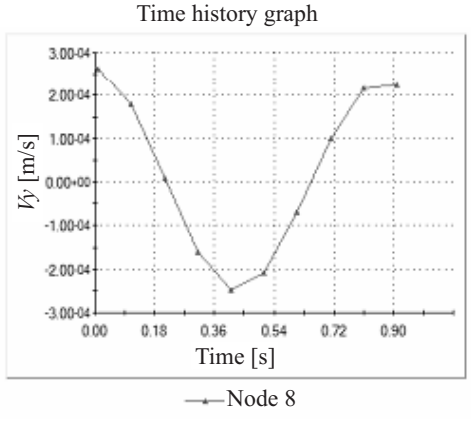

c) Response graph of the amplitude of velocity of the bogie at node 8 in the middle of mass M_1

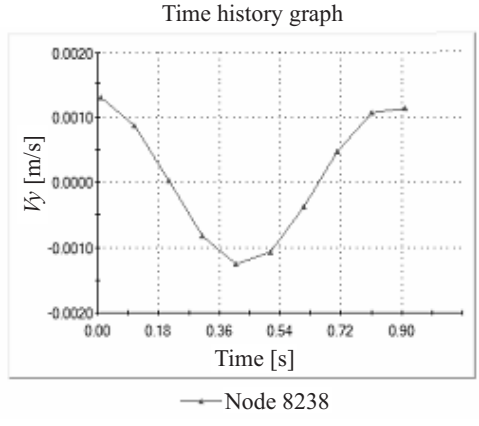

d) Response graph of the amplitude of velocity of the carriage at node 8238 in the middle of mass M_2

Fig. 4. Response graph of the dynamically scaled model

in Fig. 2 and the amplitudes of the two masses – the middle one and the top one – amplitudes of displacement and velocities are presented in Fig. 4.

4. Analysis of the results and recommendations. In this paper, an attempt is performed by the authors at modelling the shock-vibration loading in a railway carriage using a "benchmark" model vibroisolator, utilizing viscoelastic properties. A new approach is performed to the classical railway carriage suspensions, utilizing springs. Results are compared among the spring suspension model, presented in Fig. 1, and the dynamically scaled model, utilizing viscoelastic properties presented in Figs 2 and 3. Amplitudes of the displacements and

the velocities of the bogie and the carriage are presented in Fig. 4. These amplitudes of the scaled model obviously are smaller than the amplitudes of the original spring suspension model. Naturally, using a softer suspension as it is in the case of utilizing viscoelastic material-rubber at the moment, for example, ensures smaller amplitudes of the displacements and the velocities. In this way, the suspension cuts-off the amplitude of the shock impact excited by the railway and the energy of the shock is transformed into heat, released in the air. The suspension of the original spring model is much harder and the metal spring cannot react properly to the shock-vibration impact, actually there is no time to react. That is why, authors accept the viscoelastic approach in order to achieve a softer suspension and a proper reaction of the vibroisolator to the impact. On the other hand, a question arises whether it is possible for the soft viscoelastic suspension to carry on the heavy carriage full of passengers, which activity obviously can be performed by the spring suspension. The decision naturally comes with a combination of both models – the spring suspension to carry the load, while the viscoelastic vibroisolator to cut-off the shock-vibration impact. This combined model will be investigated in a future work.

5. Conclusion. In the work presented in this paper, the shock-vibrations responses of the railway vehicles are modelled using a scaled double mass dynamic model utilizing viscoelastic properties and the results derived here are compared with the results obtained using the original model. The following basic conclusions can be derived:

- The suspension which utilizes viscoelastic properties is much softer and much more compatible for shock-vibration loading;
- The parameter values of the scaled model, namely the amplitudes of displacement and velocity of the two masses are lower than in the original model, utilizing a spring suspension.

The decision naturally comes with a combination of both models – the spring suspension to carry the load, while the viscoelastic vibroisolator to cut-off the shock–vibration impact. This combined model will be investigated in a future work.

REFERENCES

[1] Karadgov T., G. Dimitrov. Carriages, Sofia, Techniks Press, 1988, p. 276 (in Bulgarian).

[2] Harris C., C. Grede. Shock and Vibration Handbook, New York, Mc Graw-Hill, 1976, p. 1211.

[3] Lagrange J. L. Mechanique analytique, Paris, 1787.

[4] Glocker C., F. Pfeiffer. Nonlinear Dynamics, **75**, 1995, No 7, 471–497.

[5] Cheshankov B. Theory of Vibrations, Sofia, TU-Sofia press, 1992, p. 254 (in Bulgarian).
[6] Penchev Ts., D. Atmadzhova. Questions of the Exploitation, the Repair and the Recycling of the carriage from the BDG Park, Reference book, Sofia, High Transport School "T. Kableshkov", 2003, p. 78 (in Bulgarian).
[7] Marinov B. Journal of Archives of Transport, **17**, 2005, No 2, 51–63.
[8] Marinov B. Journal of Mechanics, Transport, Communications, **2**, 2007, No 3, VI-7÷VI-11 (in Bulgarian).
[9] Kazakoff A., Z. Tcherneva-Popova, P. Parusheff. Journal of Mechanism and Machine Theory, **29**, 1994, No 8, 1167–1178.
[10] Kazakoff A., J. Rongong, G. Tomlinson. Proceedings of the Second International Conference Held in Swansea, 1999, 276–284.
[11] Kazakoff A., D. Karaivanov, S. Troha. Compt. rend. Acad. bulg. Sci., **60**, 2007, No 10, 1077–1084.
[12] Yunhe Yu., N. Naganathan, R. Dukkipati. Mechanism and Machine Theory, **36**, 2001, No 1, 123–142.
[13] Zlatanov Z. T. J. of Theor. And Appl. Mech., **42**, 2012, No 2, 43–54.
[14] Tsveov M., A. Kazakoff. Compt. rend. Acad. bulg. Sci., **63**, 2010, No 11, 1659–1666, ISSN 1310-1331.
[15] Marinov B. Compt. rend. Acad. bulg. Sci., **64**, 2011, No 3, 413–434, ISSN 1310-1331.
[16] Marinov B. Compt. rend. Acad. bulg. Sci., **64**, 2011, No 2, 269–276, ISSN 1310-1331.
[17] Marinov B. Shock-Wave Processes on Railway Vehicles. An Optimization, VDM Verlag Dr. Müller GmbH & Co. KG, Saarbrücken, Germany, p. 96, 2011 (ISBN: 978-3-639-32902-5).

Institute of Mechanics
Bulgarian Academy of Sciences
Acad. G. Bonchev Str., Bl. 4
1113 Sofia, Bulgaria
e-mail: alex_kazkoff@yahoo.co.uk
boicho_marinoff@yahoo.co.uk